Express Polymer Letters Vol.18, No.2 (2024) 133–143
Available online at www.expresspolymlett.com
https://doi.org/10.3144/expresspolymlett.2024.11

Research article

Experimental investigation of yield and hysteresis behaviour of an epoxy resin under cyclic compression in the large deformation regime

Jingwei Yu[1], *Christian Breite*[1], *Frederik Van Loock*[2,3], *Thomas Pardoen*[2,4], *Yentl Swolfs*[1*]

[1]Department of Materials Engineering, KU Leuven, Kasteelpark Arenberg 44, 3001 Leuven, Belgium
[2]Institute of Mechanics, Materials and Civil Engineering (iMMC), Université Catholique de Louvain, 1348 Louvain-la-Neuve, Belgium
[3]Department of Mechanical Engineering, Polymer Technology, Eindhoven University of Technology, 5600 Eindhoven, The Netherlands
[4]WEL-Research Institute, Avenue Pasteur, 6, 1300 Wavre, Belgium

Received 28 April 2023; accepted in revised form 26 October 2023

Abstract. High-performance polymers are extensively used in various applications undergoing long-term cyclic loadings. The deformation behaviour of an amorphous thermoset epoxy resin undergoing cyclic compressive loading is investigated for a range of applied deformation levels. The measurements indicate significant hysteresis upon repeated loading and unloading cycles with progressive accumulation of plastic strain. Cyclic damage leads to a reduction of the stress needed to reach the peak strain per cycle, while cyclic stiffening corresponding to an increase of elastic modulus with increasing number of cycles is observed, attributed to chain orientation effects. The dissipated energy asymptotically decreases to zero under strain-controlled cycling conditions. Interestingly, when monotonically loaded after cycling, the epoxy exhibits an increase in yield strength. This 're-yield' stress level is closely related to the selected value of the peak (unloading) strain level and increases with increasing number of loading cycles.

Keywords: *thermosetting resins, material testing, mechanical properties, fracture and fatigue, hysteresis*

1. Introduction

High-performance polymers are slowly replacing traditional materials in the automotive and aerospace industries due to their lightness, high strength, flexibility in designing, and ease of processing. Fibres are often used to reinforce the polymers and to increase their mass-normalised mechanical properties. Amorphous polymers such as crosslinked resins or thermosets are often used for composites due to their high mechanical properties over a wide range of temperatures. Polymer matrix composites are expected to stay in service for 10–50 years in structural components, which are often subjected to long-term cyclic loading. To ensure the desired lifetime and safety of these polymer-based components, the time-dependent behaviour of polymers needs to be carefully analysed under a variety of cyclic loading conditions. There is extensive experimental literature on the role of viscoelastic and viscoplastic effects on the time-dependent deformation behaviour of polymers [1–5]. Viscous effects include phenomena such as strain rate-dependency, hysteresis, relaxation, and creep. In addition, the progressive accumulation of plastic deformation under cyclic loading accelerates fatigue failure [6, 7]. Therefore, knowledge of the cyclic plastic behaviour of polymers is of utmost

---

[*]Corresponding author, e-mail: yentl.swolfs@kuleuven.be

importance for accurate structural integrity predictions of polymer components.

The following observations generally apply to high-performance amorphous polymers and some semi-crystalline thermoplastics like polypropylene (PP) and polyethylene (PE) when subjected to cyclic loading according to the experimental evidence to date:

(i) hysteresis [8–11]: the unloading and reloading branches in the stress-strain relationship are non-linear and do not follow the same path. Phase lag indicates that the deformation behaviour of polymers is time-dependent and displays viscoelasticity or/and viscoplasticity.

(ii) ratcheting effects [12–14]: significant forward and backward plastic deformation can be observed upon unloading where the reloading part of the stress-strain curve does not meet the original unloading point. The cumulative residual strain progressively develops during cyclic loading, leading to a decrease in shape recovery ratio.

(iii) energy dissipation [15–18]: the hysteresis loop indicates that external loading performs work on the polymer. The absorbed energy is dissipated into heat or changes the internal energy either by changing molecular conformations or breaking chemical bonds. The dissipated energy is closely related to stress level and loading pathways.

At the macroscopic scale, polymers exhibit linear viscoelasticity at small deformation and nonlinear viscoelastic/viscoplasticity at large deformation. Yet, most of the experimental data available on cyclic deformation behaviour of polymers are obtained at relatively low deformation levels prior to yielding. Less attention has been paid to the large deformation in the post yielding regime. Pieczyska *et al*. [10] studied the influence of strain rate on the yielding phenomena of a shape memory polymer subjected to cyclic tension. Higher stress levels and a more intense softening effect were observed at higher strain rates. Garcia-Gonzalez *et al*. [19] observed a Mullins' like effect during cyclic compression on polyvinylidene fluoride in the strain softening zone beyond yielding, where the hysteresis loops gradually stabilised at the second/third cycle. Nikoukalam and Sideris [20] conducted uniaxial cyclic compression/tension on an amorphous polyurethane with increasing applied strain levels from the pre-yielding region to the strain softening region. The envelope of the cyclic compression curve exceeds the static compression stress-strain curve when exceeding a strain of 0.05. Contrarily, the envelope of the cyclic tensile curve is much lower than the corresponding tensile stress-strain curve, demonstrating that the accumulated damage in cyclic tension is much larger compared to cyclic compression. For cyclic compression-tension, the envelope is always smaller than the tension-only and compression-only cyclic curve, indicating a damage/softening behaviour with tension-compression coupling. Colak *et al*. [21] studied the cyclic compression of pure epoxy and graphene-epoxy nanocomposite with increasing applied strain per cycle (0.06, 0.11, 0.19 and 0.27), and found that the increase in applied strain does not alter the loading-unloading curves. The inconsistency between the observation of Colak *et al*. [21] on the one hand and Nikoukalam and Sideri [20], on the other hand can be related to the influence of the applied cyclic deformation magnitude and number of loading cycles.

Recent research regarding the modelling of the cyclic response of polymers can be found in several references [22–29]. A coupled hyperelastic-viscoplastic model in Shojaei and Volgers [23] and a parallel elastic-viscoplastic network model in Qi *et al*. [27] shows capability for the investigation of a highly-crystalline and semi-crystalline polymers, respectively. Considering amorphous polymers, both the viscoelastic and viscoplastic elements are needed to accurately model the cyclic deformation behaviour. Based on the pioneering model by Haward and Thackray [30] for glassy polymers, Barriere *et al*. [29] developed a compact viscoelastic-plastic constitutive model to improve the prediction of the hysteresis loops. A pressure-dependent elastoplastic constitutive model by Melro *et al*. [31] is expanded by Rocha *et al*. [25] to capture the viscoelastic/viscoplastic behaviour of an epoxy resin. The modified model can be used in isolation or for composites subjected to cyclic loading.

The present work addresses the lack of knowledge on the cyclic behaviour of amorphous polymers when first subjected to large deformation. An improved understanding of the polymer's intrinsic behaviour upon cyclic loading in the post-yielding regime is key to predict and extend the in-service lifetime of polymer and polymer composite components (*e.g.* cyclically loaded wind turbine blades comprising fibre-reinforced polymer composite). In this study, the deformation behaviour of an epoxy resin was investigated by conducting monotonic and cyclic compressive tests. Cyclic tests were performed at different deformation levels in the post yielding regime, and the influences of applied strain level and number of loading cycles on the mechanical behaviour of the epoxy were analysed.

2. Experimental details

2.1. Material

The epoxy resin used in this study is a standard 'in-house' prepregging resin system for high-performance polymer matrix composites. The base bisphenol-A type resin (Sicomin SiPreg SR 8500) was cured by using an amine hardener (KTA 313). The Sicomin SiPreg SR 8500 exhibits low toxicity formulation and compatibility with a wide range of hardeners, offering increased flexibility in terms of working times. The viscosity of the KTA 313 cured system stays low for a long period of time, allowing easy handling and manufacturing of prepregs. This low-viscosity system is suitable for manual or mechanical impregnation of fabrics, filaments, braids, stitched reinforcements and filament winding. The main characteristics provided by the manufacturer of the SR 8500/KTA 313 system are given in Table 1.

The mixing ratio by weight of resin to hardener is 100:21. The components were first weighed separately and degassed in a vacuum oven at 70 °C for 60 min. After degassing, the resin and hardener were mixed and degassed again in a vacuum oven at room temperature for 10 min to remove all possible entrapped air bubbles. The mixture was then poured into thin glass test tubes with an inner diameter of 15.6 mm and a height of 180 mm. These tubes were thoroughly cleaned with acetone before use.

The curing cycle is a critical step for manufacturing neat epoxy resin specimens since the crosslinking reaction is exothermic and thermally activated. The curing temperature was carefully controlled to avoid forming hot spots inside the material. The tubes were placed in a holder rack to promote airflow and achieve an evenly distributed temperature in the oven. A stepwise temperature method was used for the convection oven (Memmert UF 110). The samples were cured at 120 °C for 90 min before they were cooled down to room temperature. A mould release agent (Chemlease PMR 90) was applied to the glass test tubes for easy demoulding. The slabs did not contain macroscopic voids or porosities and had a semi-transparent appearance. Based on our previous work on this resin and the same manufacturing procedure [32], we expect a void fraction of around 0.05%.

Table 1. Parameters of SR 8500/KTA 313 system from [33].

Density before curing [g/cm^3]	SR8500	1.176±0.05
	KTA313	1.13
Glass transition temperature [°C]	$T_{g,onset}$	104
	$T_{g,max}$	112
Initial viscosity after mixing [mPa·s]	20 °C	7000
	30 °C	2300
	40 °C	1000
Tension	Modulus [MPa]	3700
	Max. stress [MPa]	65
	Strain at max. stress [%]	2
Flexure	Modulus [MPa]	3700
	Max. stress [MPa]	152
	Strain at max. stress [%]	5.8

2.2. Methods

Cylindrical samples with a diameter of 12 mm and a height of 12 mm were machined from the slabs following the ASTM D695 standard. To minimise friction effect and the development of transverse confinement upon uniaxial compression experiments, the specimen faces in contact with the plates were lubricated to maintain strain uniformity longer and favour uniaxial conditions during loading. An 80 µm thick solid polytetrafluoroethylene film (PTFE-1 Teflon from Micro-Measurements/VPG) limits friction between specimen faces and fixtures over a large strain interval. The testing apparatus and specimen are shown in Figure 1.

Uniaxial compression tests were performed at room temperature on a universal testing machine (Instron 5985 with a load cell capacity of 250 kN). To evaluate the deformation behaviour of the epoxy, the following two types of tests were performed: (i) monotonic compression until failure and (ii) loading-unloading cyclic compression at different applied nominal peak strain values.

The test setup was compliance-calibrated before testing to compute the true strain from the crosshead displacement of the universal testing machine. The crosshead-based strain values agree with the average strain obtained via digital image correlation on the specimen surface. A true strain-controlled program (Bluehill) provides a constant true strain rate during the loading/unloading of specimens. For monotonic compression (i), a constant true strain rate of 0.01 s^{-1} was applied until specimen failure. For cyclic compression (ii), specimens were loaded up

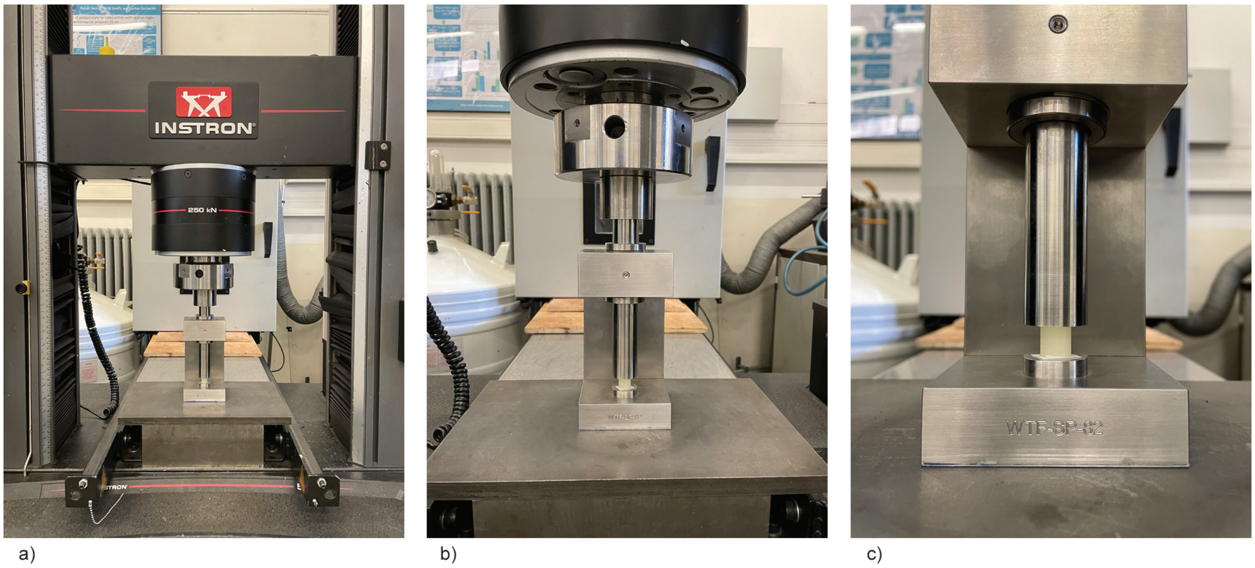

Figure 1. Testing apparatus and specimen: a) Instron 5985 testing machine; b) subpress from Wyoming Test Fixtures (WTF-SP); c) specimen and PTFE films.

to a predetermined peak strain value, then unloaded down to zero stress and subsequently reloaded up to the peak strain value. This process was repeated until a predetermined number of loading cycles was reached, followed by monotonic loading until the failure of the specimen. The entire process of loading, unloading, and reloading during cyclic compression was conducted at a constant true strain rate of 0.01 s^{-1}. The selected values of peak strain are equal to 0.10, 0.20, and 0.65.

In order to generate a stress-strain response, the assumption of plastic incompressibility is often required. The volume constancy of the highly cross-linked epoxy resin can be verified by measuring the radial and longitudinal strains on a given compression test far in the plastic regime. The measured plastic Poisson's ratio combined with an inverse FE analysis proved that the plastic incompressibility assumption was acceptable [34].

3. Results and discussion

3.1. Monotonic compressive test

Figure 2 shows the stress-strain curve of one epoxy specimen extracted from monotonic compression, where the engineering stress-strain curve is shown in Figure 2a, and the true stress-strain curve is shown in Figure 2b. The large deformation behaviour comprises four distinct regions and characteristic transition points on the curve are listed in Table 2. In region I, the epoxy exhibits elasticity-viscoelasticity without plastic deformation until reaching the yield stress $\sigma_{Y0.2\%}$ [34]. In region II, the epoxy shows a nonlinear response with a gradually decreasing stress-strain slope until the yield stress σ_U at peak force is reached. In region III, the material exhibits strain softening with a gradual reduction in true stress with increasing applied strain until the lower yield or flow stress σ_L is attained. In region IV, the strain hardening causes the true stress to rise with

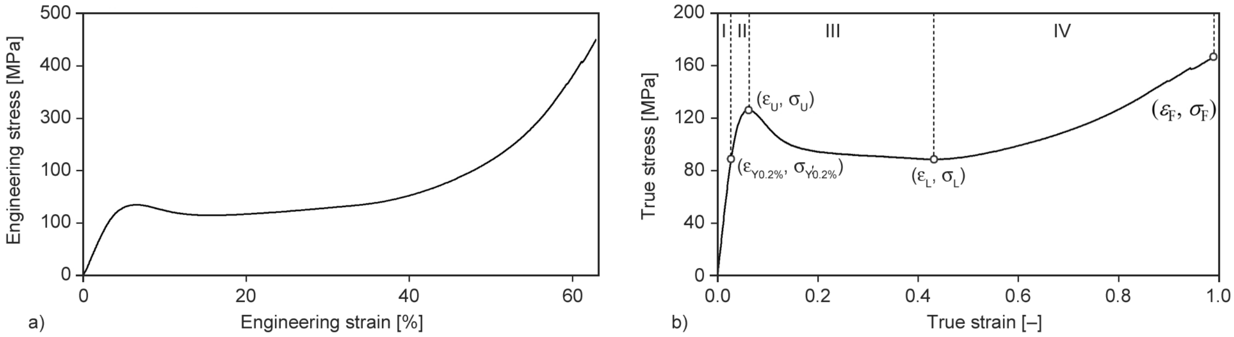

Figure 2. Stress-strain curve of the epoxy under monotonic compression at constant applied true strain rate = 0.01 s^{-1}. a) Engineering stress-strain curve, b) true stress-strain curve.

Table 2. Summary of characteristic transition points on the stress-strain response included in Figure 2.

True stress [MPa]		True strain [–]		Compressive elastic modulus [MPa]	Poisson's ratio [–]	
$\sigma_{Y0.2\%}$	86.7±1.7	$\varepsilon_{Y0.2\%}$	0.026±0.001	3573±67	elastic	0.34 [34]
σ_U	124.8±1.0	ε_U	0.061±0.001			
σ_L	87.3±0.9	ε_L	0.417±0.011		plastic	0.50 [34]
σ_F	164.7±5.7	ε_F	0.971±0.021			

increasing applied strain. When the specimen is compressed to half its original length, the engineering strain is 50%, corresponding to a true strain of 0.69. Finally, unstable crack propagation triggers a sudden drop in stress and causes ultimate failure. If the true strain reaches 1, the corresponding engineering strain is 63%.

3.2. Compressive cyclic tests

3.2.1. Hysteresis loop

The cyclic loading protocol included three deformation levels with an applied peak true strain of 0.10 (strain softening region), 0.20 (transition region), and 0.65 (strain hardening region). The hysteresis loops of the peak strain of 0.10, 0.20 and 0.65 with 1, 10, 100 and 1000 loading cycles are shown in Figure 3. The hysteresis loop is large during the first cycles and shrinks in the subsequent loading cycles, accompanied by a gradual drop in peak stress and accumulation of residual plastic strain at zero stress, see Figures 3a–3d. Single hysteresis loops for a complete loading-unloading cycle corresponding to the 1st, 10th, 100th, and 1000th cycle are shown in Figure 3e. According to the test data, the peak stress per cycle continuously decreases during cyclic loading, as shown in Figure 4a. Cyclic damage, such as polymer chain breakage and propagation of microscopic flaws termed 'microvoids' and 'microcracks' leads to the reduction of the stress needed to reach the peak strain per cycle [29]. The main molecular mechanism accounting for the residual strain upon unloading is the accumulation of conformational changes of the polymer chain segments [35]. Molecular dynamics simulations indicate that these conformational changes locally relax the stress in the epoxy network via chain kinking mechanisms such as the folding of dihedral angles between benzene rings and more flexible chain segments linked to the benzene ring [36, 37]. The residual plastic strain at zero stress rapidly grows during the first few cycles, and asymptotically approaches a steady state during long-term loading, as shown in Figure 4b. Figure 4c shows the evolution of the strain range ($\Delta\varepsilon$) during the hysteresis of one cycle. It can be observed that the value of $\Delta\varepsilon$ decreases with increasing cycles.

3.2.2. Cyclic stiffening

The value of the normalised elastic modulus is plotted as a function of the number of cycles, see Figure 4d. The value of the elastic modulus corresponds to the average slope of the linear part of the stress-strain curve during loading. Note that we report the modulus values based on the reloading part of the cycle since reverse plasticity during unloading may lead to elastic recovery, which may increase the apparent elastic modulus [12, 38]. The increase in elastic modulus with the number of cycles indicates that damage accumulation must be accompanied by another mechanism that induces 'cyclic stiffening' (the term 'cyclic hardening' is avoided to prevent confusion with the kinematic hardening effect appearing in the ratcheting of metals). Similar phenomena were reported by Drozdov and Dusunceli [39], who showed that the hysteresis loop rotates counterclockwise with the increasing number of uniaxial tensile loading cycles on semi-crystalline PP. Smerdova *et al*. [40] also observed an increasing value of the reloading modulus during cyclic indentation measurements on epoxy, polyethylene and polymethyl methacrylate. Molecular dynamics simulations reveal that chain segments of the amorphous epoxy resin were redistributed under cyclic compression and rearranged perpendicularly to the loading direction, *i.e.*, the segments were contracted in the loading direction and expanded along the non-loading direction [41]. This process causes a more ordered array of chain segments with higher load-bearing capacity, resulting in an increase in the elastic modulus [42]. As shown in Figure 4d, after the first loading/unloading process, the elastic modulus of all samples showed a decrease compared to the initial value. With the increasing loading cycles, the elastic modulus exhibits a slight drop in the first few cycles and grows until the end of the test for peak strain of 0.10, while for peak

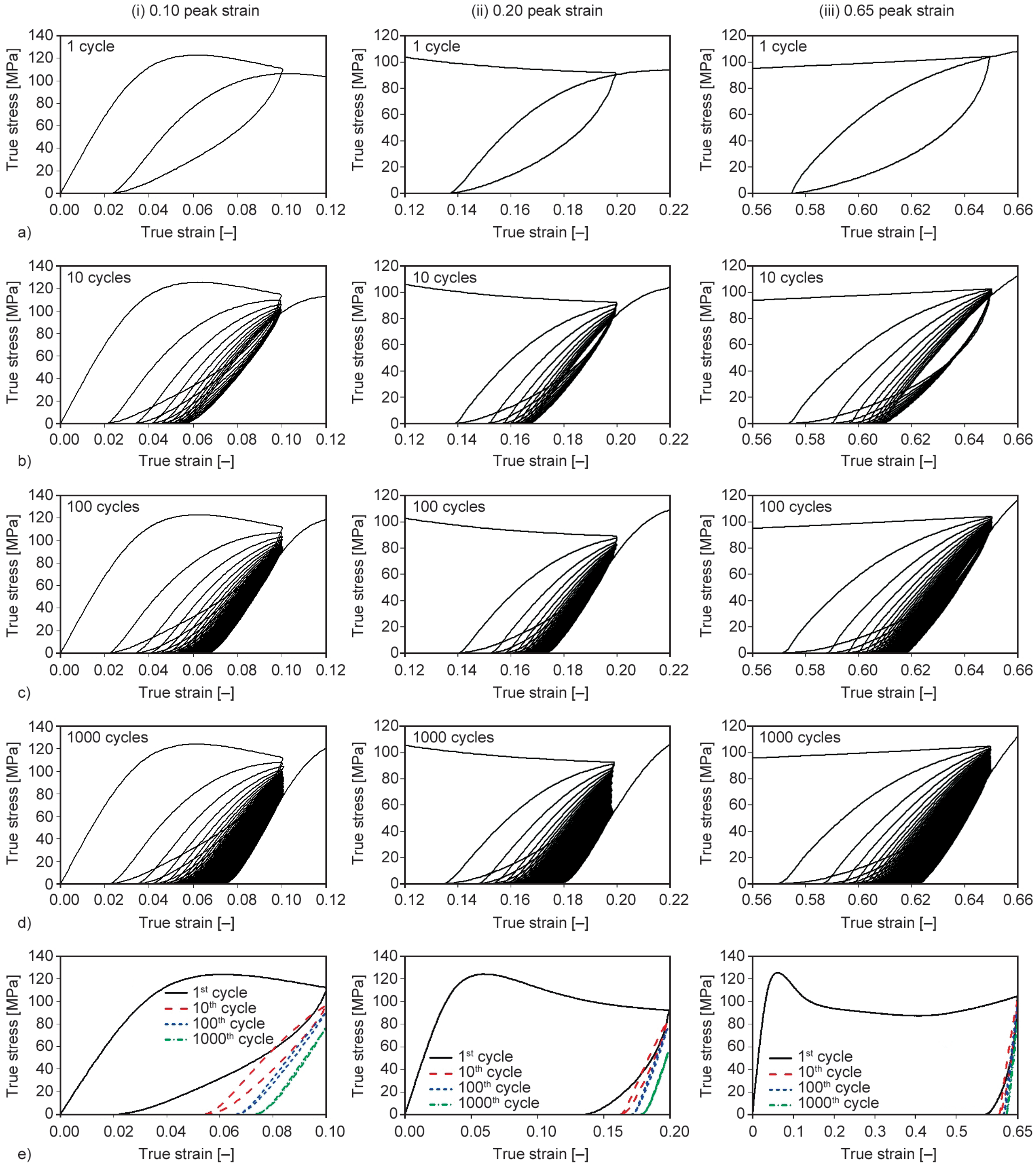

Figure 3. Hysteresis loop of i) 0.10, ii) 0.20 and iii) 0.65 peak strains for a) 1 cycle, b) 10 cycles, c) 100 cycles and d) 1000 cycles; e) single loop.

strain of 0.20 and 0.65, the elastic modulus gradually increases until reaching their peak value. A cyclic stable state was observed for a peak strain of 0.65; the elastic modulus becomes close to independent of the cycle number when this number exceeds 300. For a peak strain value of 0.20, the elastic modulus rapidly drops around 900 cycles. The evolution of elastic modulus may be understood as a competition between cyclic stiffening and damage mechanisms. When damage plays a key role during the loading process, the increase in elastic modulus induced by the alignment of chain segments is low, so it decreases driven by the propagation of microscopic flaws or chain breakages. When the influence of progressive damage is of secondary importance, an increase in elastic modulus is observed.

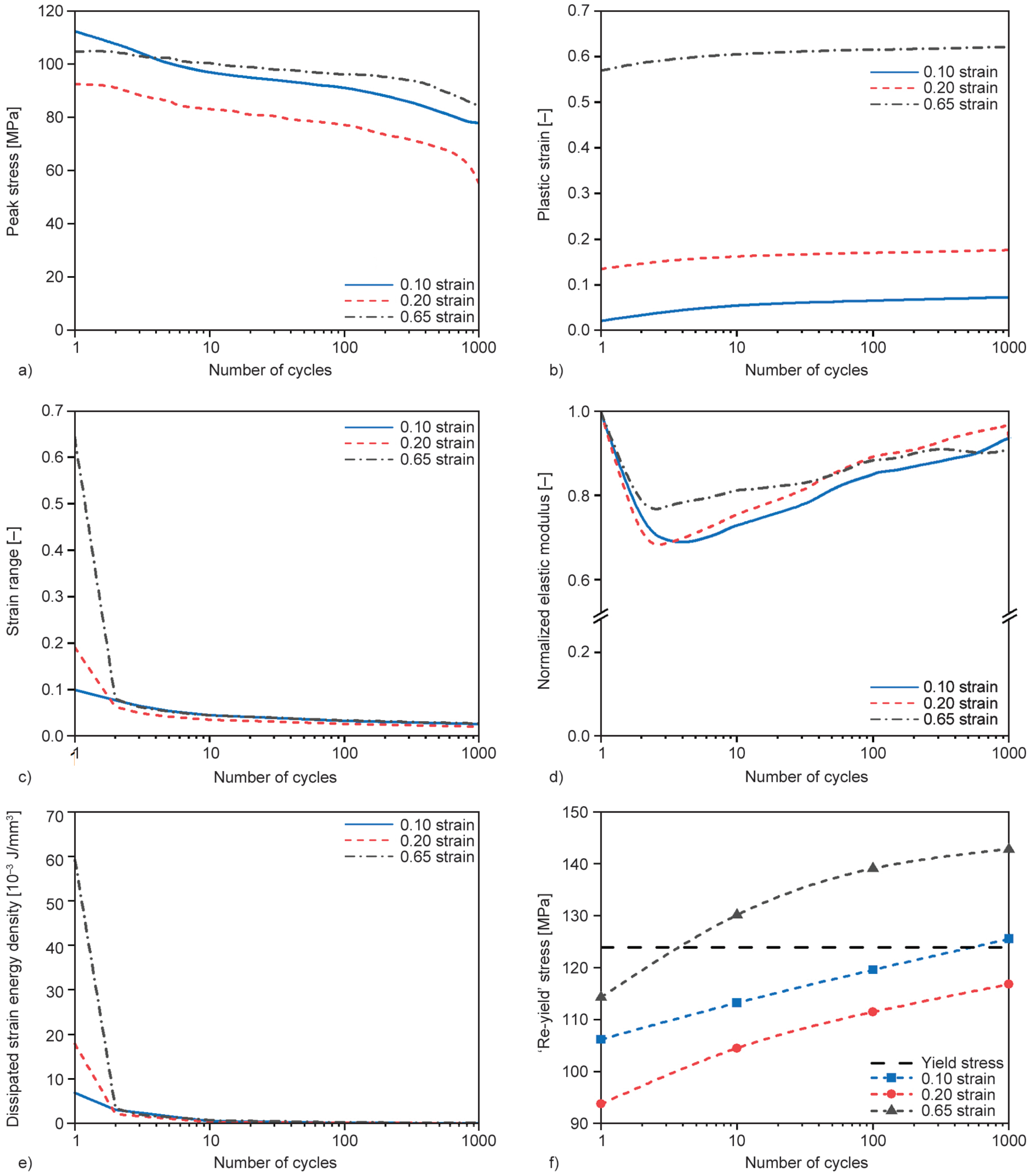

Figure 4. The evolution of a) peak stress, b) plastic strain, c) strain range, d) normalised elastic modulus, e) dissipated strain energy density per cycle, and f) 're-yield' stress as a function of the number of loading cycles compared to the nominal value of the yield strength prior to cyclic loading.

3.2.3. Non-linearity upon unloading

Figure 4e shows the area of the hysteresis loop, which represents the dissipated energy per unit volume (strain energy density) during a whole cycle. It is shown that the dissipated strain energy density drops in the first few cycles and asymptotically approaches close to zero during long-term cyclic loading. At this point, the epoxy follows a model of elastic material behaviour. The plastic deformation of a polymer material element is accompanied by the generation of a highly heterogeneous internal stress distribution; this is related to local stress-biased and thermally-activated permanent molecular rearrangements (*e.g.* via collective kinking of chain segments). These conformational changes result in isolated increments of shear of a group of atomics in molecular segments. Such mechanisms can be modelled via the 'Shear Transformation Zone' (STZ) framework originally developed for metallic glasses by Argon and co-workers [43–45]. Regions with lower activation energy barriers (due to the specific local molecular organisation) are more likely to undergo a transformation – atomic rearrangement. Hence, when unloading starts, some regions of the polymer are in a high forward stress state while other regions are in a lower forward or even backward stress state. As the macroscopic load is lowered, the zones with backward stresses can reach the threshold for backward activation of STZs and produce reverse plasticity, even though the macroscopic stress state is still forward. This phenomenon is also commonly seen in metals and known as the Bauschinger effect (although it is not often seen with such amplitude in metals) and usually requires macroscopic backward stress conditions. In polymers, all these phenomena are time-dependent as the STZs are thermally activated. It was found by Chevalier *et al.* [12] that the activation of STZs tends to re-homogenise the internal stress during creep, with a significant decrease in the back stress upon unloading. The present results fully agree with Chevalier *et al.*'s [12] finding. The cyclic load applied in the present study involves a net positive mean stress that leads to creep over time, which homogenises the internal stress state and reduces the non-linearity during cycling.

3.2.4. The 're-yield' stress

After cycling, the epoxy specimen was loaded up to failure at a constant strain rate of 0.01 s^{-1}. Interestingly, the envelope of the cyclic curve exceeds the monotonic compressive curve, and a 're-yield' point was observed after cyclic loading, as shown in Figure 5. Beyond the 're-yield' point, the epoxy exhibits softening behaviour again. This phenomenon was observed for a peak cyclic strain in the softening region (0.10 strain), in the transition region (0.20 strain), and in the strain hardening region (0.65 strain). The 're-yield' stress value increases with an increasing number of loading cycles and may even exceed the nominal yield stress, as shown in Figure 4f. These observations suggest that cyclic unloading-loading in the large deformation behaviour accelerates the physical ageing of the epoxy. Kinetics of physical ageing are dictated by the rate of molecular conformational changes [46]; these can be accelerated by temperature and applied stress [47–50]. Chain orientation effects may also contribute to the increase in re-yield stress with increasing cycles [9, 42, 51], which may explain the strong sensitivity of the dependence of the re-yield stress upon cycle number to the selected peak strain value, see Figure 4f. The detailed molecular origin behind the increase of the apparent yield stress upon cyclic loading is not

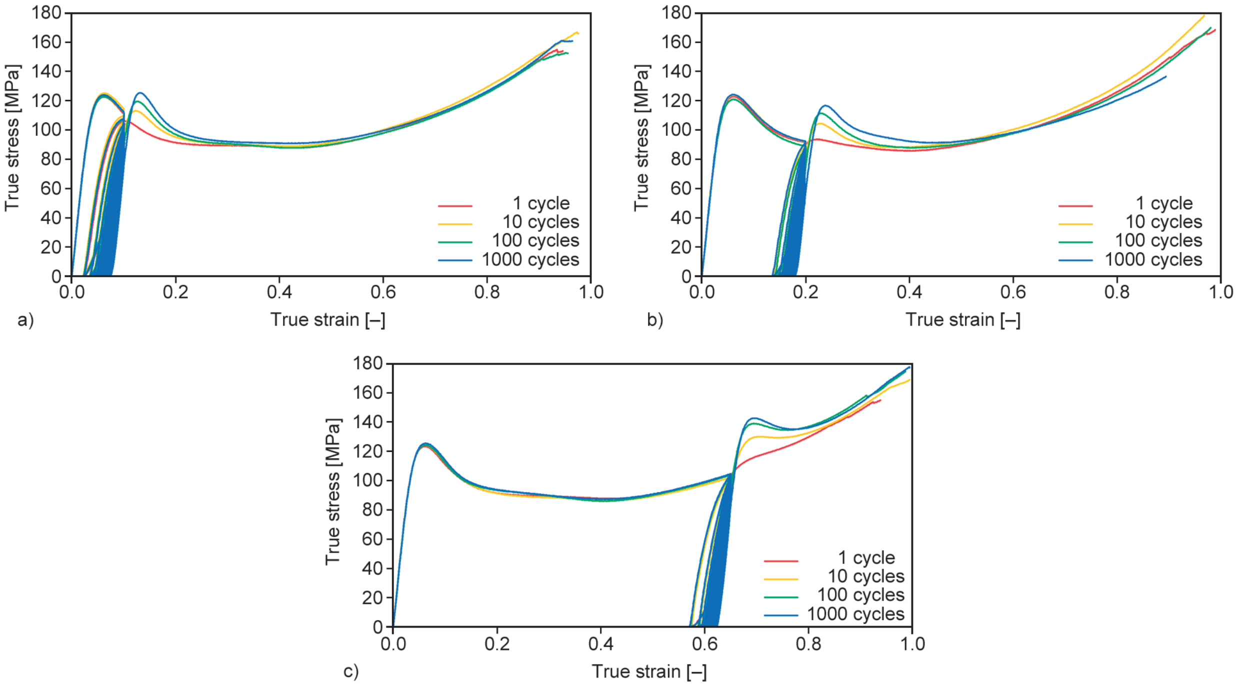

Figure 5. True stress-strain curves for a) 0.10, b) 0.20, and c) 0.65 applied peak strain.

completely understood to the best of the authors' knowledge. It is hoped that the measurement data in Figure 4f supporting this observation will motivate the use and development of specialised atomistic [51, 52] and/or mesoscale [12, 53] models aiming to understand the molecular picture associated with the apparent accelerated physical ageing in the large deformation regime. This more detailed understanding is of technological relevance as the ageing of polymer glasses is typically associated with an increased strain softening, which may lead to the acceleration of polymer component failure due to the localisation of material flow [54]. In addition, we note that a large amount of developed (phenomenological) constitutive continuum models for glassy polymers struggle to capture more complex deformation behaviour phenomena related to the development of a heterogeneous stress field at the nano-to-microscale during large deformation (*i.e.* Bauschinger, rate reversal and rate switching effects) [12, 55, 56]. The novel experimental findings on cyclic loading in the large deformation regime, summarised in Figures 3–5 could be used as an additional benchmark for further development and comparison of these models.

4. Conclusions

In this paper, the cyclic behaviour of a highly crosslinked amorphous thermoset epoxy resin was investigated through a series of uniaxial compression tests, including monotonic compression tests and cyclic compression tests at different applied unloading peak strain levels in the large deformation regime. During cyclic loading, the epoxy exhibits hysteresis with progressive accumulation of plastic strain and cyclic damage associated with a decreasing peak stress. Cyclic stiffening is observed via the increase in the elastic modulus upon reloading. The dissipated energy per cycle drops rapidly with the increasing number of cycles during the first few cycles and gradually reduces to zero, leading to a 'model elastic' material response upon unloading with no visible kinematic hardening effect.

A 're-yield' point was observed when monotonically re-loading the epoxy after cyclic loading. The 're-yield' stress value increases with an increasing number of loading cycles, and it can even exceed the nominal yield strength observed prior to cycling. These novel experimental findings suggest that cyclic unloading-loading in the large deformation regime accelerates the physical ageing of the epoxy.

Acknowledgements

To carry out this research, Christian Breite would like to acknowledge funding received from the European Union's Horizon 2020 research and innovation programme under the Marie Skłodowska-Curie grant agreement No 722626 (FiBreMoD) and from the Research Foundation – Flanders (FWO) under grant agreement No 1231322N (COCOMI).

References

[1] Drozdov A. D., de C. Christiansen J.: Viscoelasticity and viscoplasticity of semicrystalline polymers: Structure-property relations for high-density polyethylene. Computational Materials Science, **39**, 729–751 (2007). https://doi.org/10.1016/j.commatsci.2006.09.001

[2] Yu C., Kang G., Lu F., Zhu Y., Chen K.: Viscoelastic-viscoplastic cyclic deformation of polycarbonate polymer: Experiment and constitutive model. Journal of Applied Mechanics, **83**, 041002 (2016). https://doi.org/10.1115/1.4032374

[3] Xia Z., Shen X., Ellyin F.: Cyclic interaction between normal and shear stresses of an epoxy polymer-experiments and model predictions. Polymer Engineering and Science, **50**, 919–928 (2010). https://doi.org/10.1002/pen.21610

[4] Zhang Z., Chen X.: Multiaxial ratcheting behavior of PTFE at room temperature. Polymer Testing, **28**, 288–295 (2009). https://doi.org/10.1016/j.polymertesting.2008.12.012

[5] Shen X., Xia Z., Ellyin F.: Cyclic deformation behavior of an epoxy polymer. Part I: Experimental investigation. Polymer Engineering and Science, **44**, 2240–2246 (2004). https://doi.org/10.1002/pen.20251

[6] Tao G., Xia Z.: Ratcheting behavior of an epoxy polymer and its effect on fatigue life. Polymer Testing, **26**, 451–460 (2007). https://doi.org/10.1016/j.polymertesting.2006.12.010

[7] Janssen R. P. M., de Kanter D., Govaert L. E., Meijer H. E. H: Fatigue life predictions for glassy polymers: A constitutive approach. Macromolecules, **41**, 2520–2530 (2008). https://doi.org/10.1021/ma071273i

[8] Kästner M., Obst M., Brummund J., Thielsch K., Ulbricht V.: Inelastic material behavior of polymers – Experimental characterization, formulation and implementation of a material model. Mechanics of Materials, **52**, 40–57 (2012). https://doi.org/10.1016/j.mechmat.2012.04.011

[9] Xu T., Li G.: Cyclic stress-strain behavior of shape memory polymer based syntactic foam programmed by 2-D stress condition. Polymer, **52**, 4571–4580 (2011). https://doi.org/10.1016/j.polymer.2011.08.005

[10] Pieczyska E. A., Staszczak M., Kowalczyk-Gajewska K., Maj M., Golasiński K., Golba S., Tobushi H., Hayashi S.: Experimental and numerical investigation of yielding phenomena in a shape memory polymer subjected to cyclic tension at various strain rates. Polymer Testing, **60**, 333–342 (2017).
https://doi.org/10.1016/j.polymertesting.2017.04.014

[11] Yu K., Li H., McClung A. J. W., Tandon G. P., Baur J. W., Qi H. J.: Cyclic behaviours of amorphous shape memory polymers. Soft Matter, **12**, 3234–3245 (2016).
https://doi.org/10.1039/C5SM02781K

[12] Chevalier J., Brassart L., Lani F., Bailly C., Pardoen T., Morelle X. P.: Unveiling the nanoscale heterogeneity controlled deformation of thermosets. Journal of the Mechanics and Physics of Solids, **121**, 432–446 (2018).
https://doi.org/10.1016/j.jmps.2018.08.014

[13] Drozdov A. D., de C. Christiansen J.: Cyclic viscoelastoplasticity of polypropylene/nanoclay hybrids. Computational Materials Science, **53**, 396–408 (2012).
https://doi.org/10.1016/j.commatsci.2011.09.004

[14] Zrida M., Laurent H., Rio G., Pimbert S., Grolleau V., Masmoudi N., Bradai C.: Experimental and numerical study of polypropylene behaviour using an hyper-visco-hysteresis constitutive law. Computational Materials Science, **45**, 516–527 (2009).
https://doi.org/10.1016/j.commatsci.2008.11.017

[15] Drozdov A. D., de C. Christiansen J.: Cyclic viscoplasticity of high-density polyethylene: Experiments and modeling. Computational Materials Science, **39**, 465–480 (2007).
https://doi.org/10.1016/j.commatsci.2006.07.014

[16] Li C., Jaramillo E., Strachan A.: Molecular dynamics simulations on cyclic deformation of an epoxy thermoset. Polymer, **54**, 881–890 (2013).
https://doi.org/10.1016/j.polymer.2012.12.007

[17] Liu J., Qi H.: Dissipated energy function, hysteresis and precondition of a viscoelastic solid model. Nonlinear Analysis: Real World Applications, **11**, 907–912 (2010).
https://doi.org/10.1016/j.nonrwa.2009.01.033

[18] da Costa Mattos H. S., de Abreu Martins S.: Plastic behaviour of an epoxy polymer under cyclic tension. Polymer Testing, **32**, 1–8 (2013).
https://doi.org/10.1016/j.polymertesting.2012.08.009

[19] Garcia-Gonzalez D., Garzon-Hernandez S., Rusinek A., Bernier R., Arias A.: Low temperature mechanical behaviour of PVDF: Cryogenic pre-treatment, quasi-static, cyclic and dynamic experimental testing and modelling. Mechanics of Materials, **147**, 103436 (2020).
https://doi.org/10.1016/j.mechmat.2020.103436

[20] Nikoukalam M. T., Sideris P.: Experimental characterization and constitutive modeling of polyurethanes for structural applications, accounting for damage, hysteresis, loading rate and long term effects. Engineering Structures, **198**, 109462 (2019).
https://doi.org/10.1016/j.engstruct.2019.109462

[21] Colak O. U., Uzunsoy D., Bahlouli N., Francart C.: Experimental investigation of oligo cyclic compression behavior of pure epoxy and graphene-epoxy nanocomposites. Polymer Bulletin, **78**, 6935–6952 (2021).
https://doi.org/10.1007/s00289-020-03453-4

[22] Jiang C. K., Jiang H., Zhang J. W., Kang G. Z.: A viscoelastic–plastic constitutive model for uniaxial ratcheting behaviors of polycarbonate. Polymer Engineering and Science, **55**, 2559–2565 (2015).
https://doi.org/10.1002/pen.24148

[23] Shojaei A. K., Volgers P.: A coupled hyperelastic-plastic-continuum damage model for studying cyclic behavior of unfilled engineering polymers. International Journal of Fatigue, **107**, 33–39 (2018).
https://doi.org/10.1016/j.ijfatigue.2017.10.006

[24] Holopainen S., Barriere T.: Modeling of mechanical behavior of amorphous solids undergoing fatigue loadings, with application to polymers. Computers and Structures, **199**, 57–73 (2018).
https://doi.org/10.1016/j.compstruc.2018.01.010

[25] Rocha I. B. C. M., van der Meer F. P., Raijmaekers S., Lahuerta F., Nijssen R. P. L., Sluys L. J.: Numerical/experimental study of the monotonic and cyclic viscoelastic/viscoplastic/fracture behavior of an epoxy resin. International Journal of Solids and Structures, **168**, 153–165 (2019).
https://doi.org/10.1016/j.ijsolstr.2019.03.018

[26] Uchida M., Wakuda R., Kaneko Y.: Evaluation and modeling of mechanical behaviors of thermosetting polymer under monotonic and cyclic tensile tests. Polymer, **174**, 130–142 (2019).
https://doi.org/10.1016/j.polymer.2019.04.064

[27] Qi Z., Hu N., Li G., Zeng D., Su X.: Constitutive modeling for the elastic-viscoplastic behavior of high density polyethylene under cyclic loading. International Journal of Plasticity, **113**, 125–144 (2019).
https://doi.org/10.1016/j.ijplas.2018.09.010

[28] Matsubara S., Terada K., Maeda R., Kobayashi T., Murata M., Sumiyama T., Furuichi K., Nonomura C.: Viscoelastic-viscoplastic combined constitutive model for glassy amorphous polymers under loading/unloading/no-load states. Engineering Computations, **37**, 1703–1735 (2020).
https://doi.org/10.1108/EC-05-2019-0197

[29] Barriere T., Gabrion X., Holopainen S.: A compact constitutive model to describe the viscoelastic-plastic behaviour of glassy polymers: Comparison with monotonic and cyclic experiments and state-of-the-art models. International Journal of Plasticity, **122**, 31–48 (2019).
https://doi.org/10.1016/j.ijplas.2019.05.010

[30] Haward R. N., Thackray G.: The use of a mathematical model to describe isothermal stress-strain curves in glassy thermoplastics. Proceedings of the Royal Society Series A: Mathematical and Physical Sciences, **302**, 453–472 (1968).
https://doi.org/10.1098/rspa.1968.0029

[31] Melro A. R., Camanho P. P., Andrade Pires F. M., Pinho S. T.: Micromechanical analysis of polymer composites reinforced by unidirectional fibres: Part I – Constitutive modelling. International Journal of Solids and Structures, **50**, 1897–1905 (2013).
https://doi.org/10.1016/j.ijsolstr.2013.02.009

[32] Rojek J., Breite C., Swolfs Y., Laiarinandrasana L.: Void growth measurement and modelling in a thermosetting epoxy resin using SEM and tomography techniques. Continuum Mechanics and Thermodynamics, **32**, 471–488 (2020).
https://doi.org/10.1007/s00161-020-00865-5

[33] Sicomin: SiPreg SR8500/KTA31x, Epoxy systems for ‘in-house’ prepregging. Technical datasheet (2014).

[34] Morelle X. P., Chevalier J., Bailly C., Pardoen T., Lani F.: Mechanical characterization and modeling of the deformation and failure of the highly crosslinked RTM6 epoxy resin. Mechanics of Time-Dependent Materials, **21**, 419–454 (2017).
https://doi.org/10.1007/s11043-016-9336-6

[35] Jatin, Sudarkodi V., Basu S.: Investigations into the origins of plastic flow and strain hardening in amorphous glassy polymers. International Journal of Plasticity, **56**, 139–155 (2014).
https://doi.org/10.1016/j.ijplas.2013.11.007

[36] Sundararaghavan V., Kumar A.: Molecular dynamics simulations of compressive yielding in cross-linked epoxies in the context of Argon theory. International Journal of Plasticity, **47**, 111–125 (2013).
https://doi.org/10.1016/j.ijplas.2013.01.004

[37] Park H., Kim B., Choi J., Cho M.: Influences of the molecular structures of curing agents on the inelastic-deformation mechanisms in highly-crosslinked epoxy polymers. Polymer, **136**, 128–142 (2018).
https://doi.org/10.1016/j.polymer.2017.12.055

[38] Shuman D. J., Costa A. L. M., Andrade M. S.: Calculating the elastic modulus from nanoindentation and microindentation reload curves. Materials Characterization, **58**, 380–389 (2007).
https://doi.org/10.1016/j.matchar.2006.06.005

[39] Drozdov A. D., Dusunceli N.: Cyclic deformations of polypropylene with a strain-controlled program. Polymer Engineering and Science, **52**, 2316–2326 (2012).
https://doi.org/10.1002/pen.23188

[40] Smerdova O., Pecora M., Gigliotti M.: Cyclic indentation of polymers: Instantaneous elastic modulus from reloading, energy analysis, and cyclic creep. Journal of Materials Research, **34**, 3688–3698 (2019).
https://doi.org/10.1557/jmr.2019.289

[41] Park H., Chung I., Cho M.: Effect of molecular structure of curing agents on cyclic creep in highly crosslinked epoxy polymers. Journal of Polymer Science, **58**, 1617–1631 (2020).
https://doi.org/10.1002/pol.20200130

[42] Drozdov A. D.: Cyclic strengthening of polypropylene under strain-controlled loading. Materials Science and Engineering: A, **528**, 8781–8789 (2011).
https://doi.org/10.1016/j.msea.2011.08.019

[43] Argon A. S.: Plastic deformation in metallic glasses. Acta Metallurgica, **27**, 47–58 (1979).
https://doi.org/10.1016/0001-6160(79)90055-5

[44] Argon A. S., Shi L. T.: Development of visco-plastic deformation in metallic glasses. Acta Metallurgica, **31**, 499–507 (1983).
https://doi.org/10.1016/0001-6160(83)90038-X

[45] Bulatov V. V., Argon A. S.: A stochastic model for continuum elasto-plastic behavior. I. Numerical approach and strain localization. Modelling and Simulation in Materials Science and Engineering, **2**, 167 (1994).
https://doi.org/10.1088/0965-0393/2/2/001

[46] Capaldi F. M., Boyce M. C., Rutledge G. C.: Enhanced mobility accompanies the active deformation of a glassy amorphous polymer. Physical Review Letters, **89**, 175505 (2002).
https://doi.org/10.1103/PhysRevLett.89.175505

[47] Struik L. C. E.: Physical aging in amorphous glassy polymers. Annals of the New York Academy of Sciences, **279**, 78–85 (1976).
https://doi.org/10.1111/j.1749-6632.1976.tb39695.x

[48] Senden D. J. A., van Dommelen J. A. W., Govaert L. E.: Physical aging and deformation kinetics of polycarbonate. Journal of Polymer Science Part B: Polymer Physics, **50**, 1589–1596 (2012).
https://doi.org/10.1002/polb.23161

[49] Clarijs C. C. W. J., Kanters M. J. W., van Erp M. J., Engels T. A. P., Govaert L. E.: Predicting plasticity-controlled failure of glassy polymers: Influence of stress-accelerated progressive physical aging. Journal of Polymer Science Part B: Polymer Physics, **57**, 1300–1314 (2019).
https://doi.org/10.1002/polb.24870

[50] Pastukhov L. V., Kanters M. J. W., Engels T. A. P., Govaert L. E.: Physical background of the endurance limit in poly(ether ether ketone). Journal of Polymer Science, **58**, 716–736 (2020).
https://doi.org/10.1002/pol.20190091

[51] Liu A. Y-H., Rottler J.: Aging under stress in polymer glasses. Soft Matter, **6**, 4858–4862 (2010).
https://doi.org/10.1039/C0SM00318B

[52] Warren M., Rottler J.: Deformation-induced accelerated dynamics in polymer glasses. The Journal of Chemical Physics, **133**, 164513 (2010).
https://doi.org/10.1063/1.3505149

[53] van Loock F., Brassart L., Pardoen T.: Implementation and calibration of a mesoscale model for amorphous plasticity based on shear transformation dynamics. International Journal of Plasticity, **145**, 103079 (2021).
https://doi.org/10.1016/j.ijplas.2021.103079

[54] van Melick H. G. H., Govaert L. E., Meijer H. E. H.: Localisation phenomena in glassy polymers: Influence of thermal and mechanical history. Polymer, **44**, 3579–3591 (2003).
https://doi.org/10.1016/S0032-3861(03)00089-2

[55] Lin J., Qian J., Xie Y., Wang J., Xiao R.: A mean-field shear transformation zone theory for amorphous polymers. International Journal of Plasticity, **163**, 103556 (2023).
https://doi.org/10.1016/j.ijplas.2023.103556

[56] Medvedev G. A., Caruthers J. M.: A comparison of constitutive descriptions of the thermo-mechanical behavior of polymeric glasses. in ‘Polymer glasses’ (ed.: Roth C. B.) Taylor and Francis, Boca Raton, 467–552 (2016).
https://doi.org/10.4324/9781315305158